Exciton-Mott Physics in a Quasi-One-Dimensional Electron-Hole System

Takuya Yoshioka and Kenichi Asano

Department of Physics, Osaka University, Toyonaka, Osaka, 560-0043, Japan

(Received 27 July 2011; published 16 December 2011)

We investigate the correlation effect in the quasi-one-dimensional electron-hole (e-h) system under thermal equilibrium. A self-consistent screened T-matrix approximation developed here enables the description of an e-h pair under any ionization ratio, the portion of quasielectrons or quasiholes moving almost freely. Our phase diagram on the ionization ratio provides a unified description of exciton Mott physics from the low-density exciton gas towards the high-density electron-hole plasma, and predicts a first order transition at low temperature. The interband optical absorption-gain spectra are also evaluated, which succeeded in explaining semiquantitatively all aspects of the recent experimental observations in the strongly photoexcited quantum wires.

DOI: 10.1103/PhysRevLett.107.256403 PACS numbers: 71.35.Lk, 71.35.Ee, 78.67.Lt

The Mott metal-insulator transition or crossover [1] is a fundamental problem in many body theory, which is indeed commonly found in various systems in different fields, e.g., electron-hole (or semimetallic) systems, doped semiconductors, transition-metal compounds, organic solids, quantum plasmas, liquid metals, ultracold atom gases, nuclear matters, and quark-gluon plasmas [2]. Nowadays, Mott physics is most intensively studied in Hubbard models, i.e., in lattice systems with short-range interaction, and its breakthrough was brought by the establishment of global phase diagrams [3]. Similarly, for many of the continuum Mott systems, the global phase diagrams lead to another breakthrough. In such cases, the long-range Coulomb interaction is expected to play a crucial role, as was argued by Mott himself [1]. This open issue is studied in this Letter by the simplest model in quasi-one-dimension (quasi-1D), which consists of an equal number of electrons and holes. We succeed in drawing the global phase diagram for the exciton Mott crossover or transition between the metallic electron-hole (e-h) plasma and insulating exciton gas on the plane of electron (or equivalently hole) density n and temperature T.

Such quasi-1D e-h systems also attract attention as candidates of highly efficient laser devices [4–10], since free-carrier theories [11,12] predict that the divergent density of states (DOS) at the band edge gives rise to the low-threshold and high-differential optical gain. However, this may no longer be valid once the interaction effect is relevant: the Mott crossover or transition [13–17], which is a prerequisite for the optical gain by the e-h plasma, might be hindered by the strong enhancement of excitonic correlation by the spatial confinement [18,19]. Further, Ref. [16] even argues the absence of the Mott crossover due to the non-Fermi-liquid nature of 1D, which, however, contradicts the most recent experimental observations [9,10]. Our global phase diagram settles this long-standing controversy, and marks a milestone in the development of quasi-1D laser devices.

The exciton Mott transition or crossover can be classified into three types. One is a crossover between exciton gas and e-h plasma [20] at high T under the variation of n, which is observed as a disappearance of the excitonic peak in the interband optical absorption spectra [21], when n exceeds the so-called Mott density. The second one is the first order phase transition accompanied by an inhomogeneous coexisting region, which is characterized by the n-independent e-h chemical potential, the sum of the electron and the hole chemical potentials, $\mu = \mu_e + \mu_h$ [22,23]. Such coexistent phase is observed in the strongly photoexcited indirect-gap semiconductors. The last one, which we call pure Mott transition, shows a discontinuity in the ionization ratio as well as μ at a critical value of n, accompanied by a hysteresis behavior. This discontinuity was observed recently in the type II quantum well [24], which is, however, only poorly examined theoretically [25].

To give a perspective of the Mott transition or crossover in quasi-1D e-h systems, we need a novel theoretical scheme which can capture all of the above three aspects of Mott physics on equal terms. The screened self-consistent T-matrix approximation is used here, in which self-energies, T matrices, and screening parameters are determined in a consistent manner. Although similar kinds of formalism were established substantially in the 1980s [26], it was applied to realistic bulk (three-dimensional) e-h systems only recently [27] due to numerical limitation.

As summarized in Fig. 1, we start from a guess of self-energies of electron and hole, and iterate the following four steps until the self-energies converge. First, the single particle Green's function, $G_a(k, \omega)$, is evaluated via the Dyson equation, where k is the wave number in the axial direction, ω is the frequency, and $a = e, h$ represent electron and hole. The chemical potential μ_a is determined in such a way that the electron-hole density calculated from $G_a(k, \omega)$ equals n. Next, we evaluate the screened Coulomb interaction potential using a quasistatic

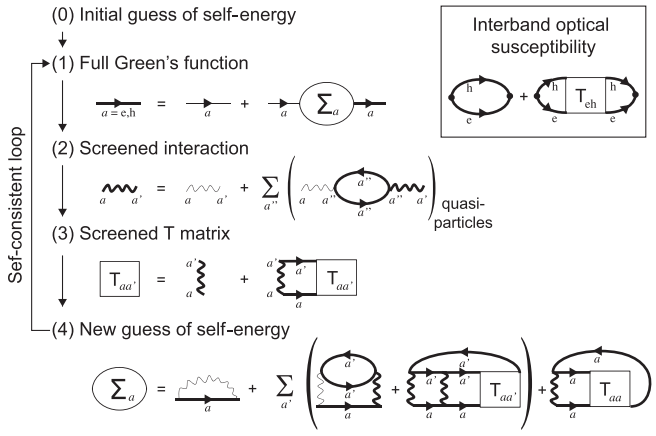

FIG. 1. Calculation scheme depicted by Feynman diagrams. Thick and thin solid lines denote full and bare single particle Green's functions, respectively, while thick and thin wavy lines represent screened and bare Coulomb interactions, respectively. Inset: Interband optical susceptibility.

plasmon-pole approximation (PPA) [13] including only the quasielectron and quasihole contributions. In fact, the screening parameter is estimated as $\kappa = (\pi k_B T)^{-1} \sum_a \int f_{a,k}(1 - f_{a,k}) dk$ with Fermi distribution functions for the quasielectron and the quasihole, $f_{a,k} = (e^{(\xi_{a,k} - \mu_a)/k_B T} + 1)^{-1}$, where $\xi_{a,k}$ is determined by solving $\mathrm{Re}[G_a^{-1}(k, \xi_{a,k} - \mu_a)] = 0$. In the third step, T matrices for e-e, h-h, and e-h scatterings are evaluated within the ladder approximation for the screened interaction. The final step is devoted to a new guess of self-energies by collecting terms depicted by the Feynman diagrams in Figure 1, step (4). The first and the second diagrams denote the Hartree-Fock and the Montroll-Ward terms, while the third and the fourth correspond to direct and exchange contributions of T matrices, respectively.

Let us briefly mention our development from the previous formulation [27]. We substitute the second-order scattering (screened Born) term in the direct T-matrix contribution with the Montroll-Ward term to avoid double counting of Feynman diagrams. We no longer need the additional screened Hartree-Fock (screened-exchange and Coulomb-hole) term since it is already considered via the Hartree-Fock and the Montroll-Ward terms. Our self-energies include the exchange contribution of T matrices.

As a realistic quasi-1D e-h system, we consider in the following a strongly photoexcited semiconductor quantum wire. There, we assume that electrons and holes can reach a quasithermal equilibrium before their recombination since the intraband relaxation time is far shorter than the interband one. In our model of wire, all electrons and holes are confined in the ground subband formed by the hard-wall potential with a rectangular cross section. The side lengths of the rectangle are set to 18.9 and 8.09 nm so as to reproduce the aspect ratio of the cross section and the quasi-1D exciton binding energy, $E_{1D} = 14$ meV, observed in the T-shape quantum wire [9,10]. We use the background dielectric constant, $\epsilon_0 = 13.74$, and the effective mass of electron and hole in the axial direction, $m_e = 0.0665 m_0$ and $m_h = 0.11 m_0$, with the electron rest mass m_0. The final results are insensitive to the geometrical form of the wire, if the energy and the length are scaled by the quasi-1D exciton binding energy E_{1D} and Bohr radius, $a_{1D} = \hbar/\sqrt{2mE_{1D}}$, respectively, where $m = m_e m_h/(m_e + m_h)$ denotes the reduced mass.

Figure 2(a) shows the phase diagram on the n-T plane as contour plots of the ionization ratio, $\alpha = (2\pi n)^{-1} \sum_a \int f_{a,k} dk$, which is the ratio of the quasielectron-hole density to the total electron-hole density n. The horizontal axis $n a_{1D}$ denotes the inverse of the r_s parameter in quasi-1D. The Mott density (dash-dotted line) indicates the vanishing of the exciton ionization energy, $E_g^* - (E_g - E_{1D}) = 0$, where E_g and $E_g^* = \xi_{e,k=0} + \xi_{h,k=0}$ denote the bare and renormalized band gaps, respectively. Note that the exciton energy is almost n independent and is given as $E_g - E_{1D}$ due to its charge neutrality.

The electrons and holes are almost fully ionized in two extreme regions, the low-n–high-T (left-upper) and the high-n–low-T (right-lower) regions. In the former region, the electrons and holes behave as classical plasma, whereas in the latter region on the right-hand side of the Mott density line, they are regarded as quantum plasma. The almost genuine exciton gas with extremely small ionization ratio is realized only at low n ($n a_{1D} \lesssim 0.5 \times 10^{-1}$) and low T ($k_B T/E_{1D} \lesssim 10^{-1}$). At even lower T, we also find a shaded region where the homogeneous thermodynamic state can no longer exist. The boundary of this region is characterized by the divergence of isothermal compressibility, $n^{-2}(\partial n/\partial \mu)_T$, which indicates the instability toward an inhomogeneity.

In the low-n and high-T region, $n\lambda_T < 0.2$, α is well evaluated by the Saha equation for the mixture of ideal gas of electrons, holes, and excitons of the lowest energy, $\alpha^2(1 - \alpha)^{-1} = (n\lambda_T)^{-1} e^{-E_{1D}/k_B T}$, where we define the thermal de Broglie wavelength as $\lambda_T = h/\sqrt{2\pi m k_B T}$. In this region, α is a monotonically decreasing function of n and an increasing function of T. As n increases, the contour lines start to deviate from a gradually increasing line of the Saha equation, bend around the dotted line, $n\lambda_T \sim 0.2$, and then follow the steep Mott density line. In the right-hand region of this dotted line, α increases drastically by n, which mainly stems from the Pauli-blocking effect. Just above the unstable region, α increases suddenly and approaches a pure Mott transition: some of the contours flow into the same point with lowering T. This singularity reflects the discontinuous change of the screening parameter as will be mentioned shortly. At around the Mott density line, α reaches unity and electrons and holes turn to fully ionized quantum plasma.

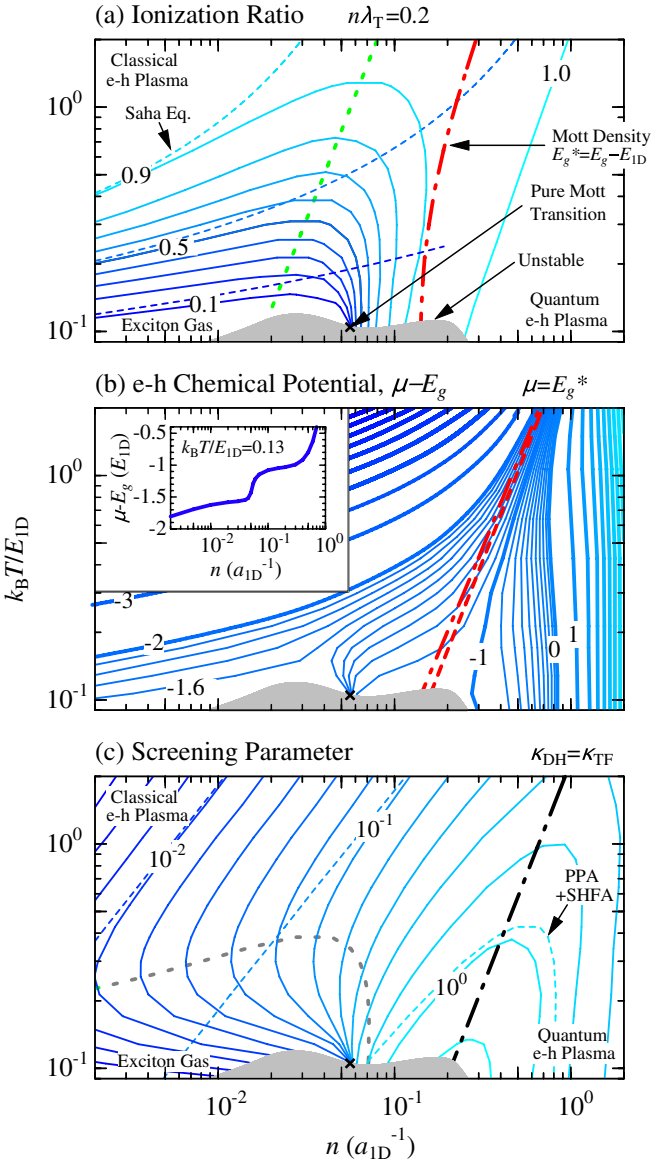

FIG. 2 (color online). Phase diagrams of a quasi-1D e-h system depicted by three contour plots on the n-T plane. Electron-hole density n and temperature T are scaled by inverse of quasi-1D exciton Bohr radius, $a_{1D}^{-1} = 1.24 \times 10^6$ cm^{-1}, and binding energy, $E_{1D} = 162$ K, respectively. Isothermal compressibility diverges on the boundary of the shaded region, in which uniform thermodynamic states are destabilized. (a) Ionization ratio α (solid lines), together with Mott density (dash-dotted line). Broken lines for $\alpha = 0.1$, 0.5, and 0.9 are calculated by the classical Saha equation. The dotted line shows the condition $n\lambda_T = 0.2$, with thermal de Broglie length, λ_T defined with the reduced mass. (b) e-h chemical potential, $\mu = \mu_e + \mu_h$, measured from E_g (solid lines). Dash-dotted and broken lines show the onset of plasma gain derived by the present and the free-carrier theories, respectively. Inset: n dependence of μ at $k_BT = 0.13E_{1D}$. (c) Screening parameter κ (solid lines) in comparison with the one calculated following Ref. [13] (broken lines). Dash-dotted line shows the condition that the Debye-Hückel and Thomas-Fermi screening parameters, κ_{FH} and κ_{TF}, are equal. Dotted line denotes contour line for $\alpha = 0.6$. Contour values are scaled by e^2/ϵ_0 with the elementary charge e.

Figure 2(b) shows the contour plot of the e-h chemical potential μ on the n-T plane. At the higher-T region ($k_BT/E_{1D} \gtrsim 0.3$), μ gradually and monotonically increases as a function of n, while at lower T several anomalies are found. One significant feature is the bundling of contour lines near the pure Mott transition point mentioned above. This indicates that μ also shows a significant increase with n around this point. Once off this point, the contour lines become quite sparse, namely, μ remains almost independent of n, which is regarded as a precursor of the unstable (inhomogeneous) phase. Consequently, μ behaves almost like a step function as shown in the inset, from the semigenuine exciton gas value to the quantum e-h plasma one [28].

The dash-dotted line describes the condition, $\mu = E_g^*$, which is the onset of the optical gain induced by the e-h plasma (plasma gain) [29]. In contrast to the complicated behavior of the $\mu - E_g$ contour lines, this $\mu = E_g^*$ shows no singularity even near the unstable region, which implies that the interaction effects on μ and E_g^* are canceled out. In fact, the $\mu = E_g^*$ line in our theory is quite close to the corresponding line drawn by the free-carrier theory (broken line), which is well approximated by $n\lambda_T = 2(m_e m_h/m^2)^{1/4} I_{-1/2}(0) = 1.21 \times (m_e m_h/m^2)^{1/4}$ with $I_{-1/2}(x)$ being the complete Fermi-Dirac integral of order $-1/2$. The present results thus guarantee that the onset of plasma gain can be safely evaluated semiqualitatively by the free-carrier theory.

Figure 2(c) is devoted to the contour of the screening parameter κ on the n-T plane. Let us first explain briefly the reference result which does not include the excitonic effect; in the quantum e-h plasma regime, the screening parameter is expected to increase with decreasing n due to the divergence of DOS at the band edge. However, if n is decreased further, the e-h system turns to the classical e-h plasma, and thus the screening parameter will be suppressed gradually as n decreases. This classical-quantum crossover is well described by $\kappa_{DH} = \kappa_{TF}$, or equivalently, $n\lambda_T = \sqrt{4M/\pi m}$ with $M = m_e + m_h$, where $\kappa_{DH} = 2n/k_BT$ and $\kappa_{TF} = 4M/\pi^2\hbar^2 n$ denote the screening parameters evaluated by the Debye-Hückel and Thomas-Fermi approximations, respectively. These two limits are interpolated by the conventional method in Ref. [13], which we call PPA + SHFA [broken lines in Fig. 2(c)]. They evaluate the screening parameter by the PPA for the fully ionized e-h plasma in which the quasielectron or quasihole energies are estimated by the screened Hartree-Fock approximation (SHFA).

Now, let us compare our results with those of PPA + SHFA. In the high ionization regime, $\alpha \gtrsim 0.6$, the screening parameter almost follows the PPA + SHFA results, which, however, breaks down once we enter the low ionization region, $\alpha \lesssim 0.6$, and the contour line bends and flows into the pure Mott transition point. The low-T–low-n region on the left-hand side of this point is a semigenuine

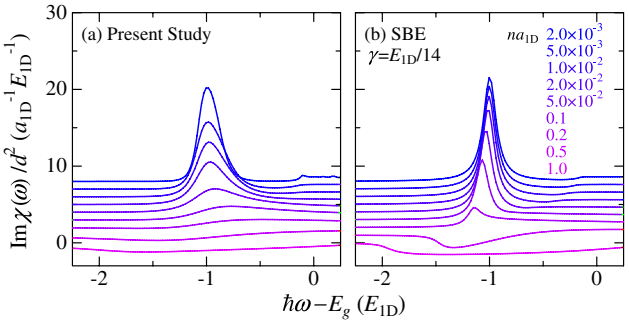

FIG. 3 (color online). (a) Interband optical absorption-gain spectra per axial length calculated at $k_B T = 0.3E_{1D} = 49.2$ K for several e-h densities. (b) Those calculated by semiconductor Bloch equation. Photon energy and dipole matrix element are denoted by $\hbar\omega$ and d, respectively.

exciton gas, which has only a small number of charged quasielectrons or quasiholes so that the screening effect is suppressed significantly. Therefore, on entering this region, the screening parameter shows an almost discontinuous or drastic change, which cannot be expressed in the conventional theory which does not take into account the excitonic effect in the screening parameter.

We finally evaluate the interband optical absorption-gain spectra per axial length as the imaginary part of the susceptibility derived from the e-h T matrix as shown in the inset of Fig. 1. We set $T = 0.3E_{1D} = 49.2$ K close to the experimental value in Ref. [10]. The exciton peak is gradually suppressed with increasing n and disappears near the Mott density, reflecting the Mott crossover. Then, one finds three distinct features. First, the plasma gain becomes relevant above the onset density [29]. Second, both the exciton peak position and the continuum onset (i.e., the renormalized band gap) remain almost unshifted at low n. Finally, one finds an intrinsic broadening caused by the intercarrier scatterings, which results in a characteristic low-energy tail. These three features are actually observed in experiments [4–10], while not fully explained by the previous theories.

The reference result calculated by the semiconductor Bloch equation (SBE) [13,17] is presented in Fig. 3(b). While the SBE reproduces the plasma gain, their exciton peak distinctly shows a redshift by n, and the intrinsic broadening is not considered: a phenomenological broadening, $\gamma = E_{1D}/14 = 1$ meV, is introduced by hand. There is another theory including the dynamical screening effect, which settles the above two problems of SBE [16]. Then, however, the optical gain is washed out and the Mott crossover never occurs. By contrast, we succeeded in reproducing semiqualitatively all these features in recent measurements [9,10] by including the ionization-ratio concept, without introducing any phenomenological fitting parameters.

To summarize, we visualized the Mott physics realized in the quasi-one-dimensional strongly photoexcited semiconductors on the global phase diagram using the self-consistent screened T-matrix approximation by properly taking into account the suppression of the screening effect by the exciton formation. We also succeeded in reproducing the interband optical absorption-gain spectra observed in recent experiments. Although a Mott crossover exists and the plasma gain does arise, the huge optical gain at the band edge expected from the free-carrier theory is suppressed by the spectral broadening caused by the intercarrier scattering. In addition to the Mott crossover at high temperature, our phase diagram predicts the unstable (inhomogeneous) region as well as pure Mott transition, which are still not detected experimentally due to the finite e-h lifetime. However, the two-peak structure found in photoluminescence measurements [9] might be a precursor of inhomogeneity found in the lowest temperature region of our phase diagram. It is a future problem to clarify whether the unstable region indicates a coexisting region or a novel inhomogeneous phase, e.g., the biexcitonic crystallization proposed by one of the authors within the bosonization scheme [30]. To answer this problem, we should include interexcitonic correlations neglected in the present framework. Although a quantum condensation of an e-h pair might take place at low temperature, no instability was found in the parameter region of our phase diagram. This is presumably because our self-energies include the e-h T-matrix contribution, properly accounting for the enhancement of the e-h pair fluctuation in low dimension.

This work is supported by KAKENHI (No. 20104010 and No. 21740231).

[1] N. F. Mott, Philos. Mag. **6**, 287 (1961).
[2] See, for example, *Metal-to-Nonmetal Transtions*, edited by R. Redmer, B. Holst, and F. Hensel (Springer, Berlin, 2010).
[3] See, for example, A. George *et al.*, Rev. Mod. Phys. **68**, 13 (1996).
[4] E. Kapon, D. M. Hwang, and R. Bhat, Phys. Rev. Lett. **63**, 430 (1989).
[5] W. Wegscheider *et al.*, Phys. Rev. Lett. **71**, 4071 (1993).
[6] R. Ambigapathy *et al.*, Phys. Rev. Lett. **78**, 3579 (1997).
[7] Y. Hayamizu *et al.*, Appl. Phys. Lett. **81**, 4937 (2002).
[8] T. Guillet *et al.*, Phys. Rev. B **67**, 235324 (2003).
[9] Y. Hayamizu *et al.*, Phys. Rev. Lett. **99**, 167403 (2007).
[10] M. Yoshita *et al.* (unpublished).
[11] Y. Arakawa and H. Sakaki, Appl. Phys. Lett. **40**, 939 (1982).
[12] M. Asada, Y. Miyamoto, and Y. Suematsu, Jpn. J. Appl. Phys. **24**, L95 (1985).
[13] S. Benner and H. Haug, Europhys. Lett. **16**, 579 (1991).
[14] F. Tassone and C. Piermarocchi, Phys. Rev. Lett. **82**, 843 (1999); C. Piermarocchi and F. Tassone, Phys. Rev. B **63**, 245308 (2001).

[15] S. Das Sarma and D. W. Wang, Phys. Rev. Lett. **84**, 2010 (2000).
[16] D. W. Wang and S. Das Sarma, Phys. Rev. B **64**, 195313 (2001).
[17] P. Huai *et al.*, Jpn. J. Appl. Phys. **46**, L1071 (2007).
[18] R. Loudon, Am. J. Phys. **27**, 649 (1959).
[19] T. Ogawa and T. Takagahara, Phys. Rev. B **43**, 14 325 (1991).
[20] R. Zimmermann *et al.*, Phys. Status Solidi B **90**, 175 (1978).
[21] S. Schmitt-Rink, J. Löwenau, and H. Haug, Z. Phys. B **47**, 13 (1982).
[22] W. F. Brinkmann and T. M. Rice, Phys. Rev. B **7**, 1508 (1973).
[23] H. Haug, Z. Phys. B **24**, 351 (1976).
[24] M. Stern *et al.*, Phys. Rev. Lett. **100**, 256402 (2008).
[25] D. W. Snoke and J. D. Crawford, Phys. Rev. E **52**, 5796 (1995).
[26] R. Zimmermann and H. Stoltz, Phys. Status Solidi B **131**, 151 (1985); H. Stoltz and R. Zimmermann, *ibid.* **94**, 135 (1979).
[27] N. H. Kwong, G. Rupper, and R. Binder, Phys. Rev. B **79**, 155205 (2009).
[28] Phase transition between a paired electron gas and an electron liquid is discussed in the attractive Hubbard model [M. Capone, C. Castellani, and M. Grilli, Phys. Rev. Lett. **88**, 126403 (2002)], where one finds the phase coexistence (flattening of μ) by varying the filling factor and the discontinuous change of double occupancy (interpreted as $1 - \alpha$) by varying the interaction. Our n varies both the filling and the interaction strength, thus the behavior of μ and α against n is similar with their results, although the two models differ qualitatively.
[29] The Kubo-Martin-Schwinger relation shows that optical gain appears at photon energies below μ. Thus, plasma gain can exist only at $E_g^* < \mu$. Nevertheless, the low-energy spectral tails allows small gain even at $E_g^* > \mu$, i.e., below the onset density, which is called excitonic gain [14].
[30] K. Asano and T. Ogawa, J. Lumin. **112**, 200 (2005).